Materials for Energy Converstion

Workshop 3: Batteries and Fuel Cells

IPAM: November 5, 2013

Network Structures in Amphiphilic Materials

K. Promislow, A. Christlieb, S. Dai, and N. Gavish

MICHIGAN STATE UNIVERSITY

MICHIGAN STATE UNIVERSITY

Goals

- Develop a novel continuum framework for the network formation in amphiphilic mixtures
- Incorporate the role of solvent quality, functional groups, counter-ions
- Propose connections between charge transport and network morphology
- All within the context of a "minimal system" which respects a governing energy via an Onsager relations.

Part I A pragmatic approach to interfacial energy
Part II Connections to more traditional electrostatic energy formulations

Role of Solvent in Cast-Driven Morphology

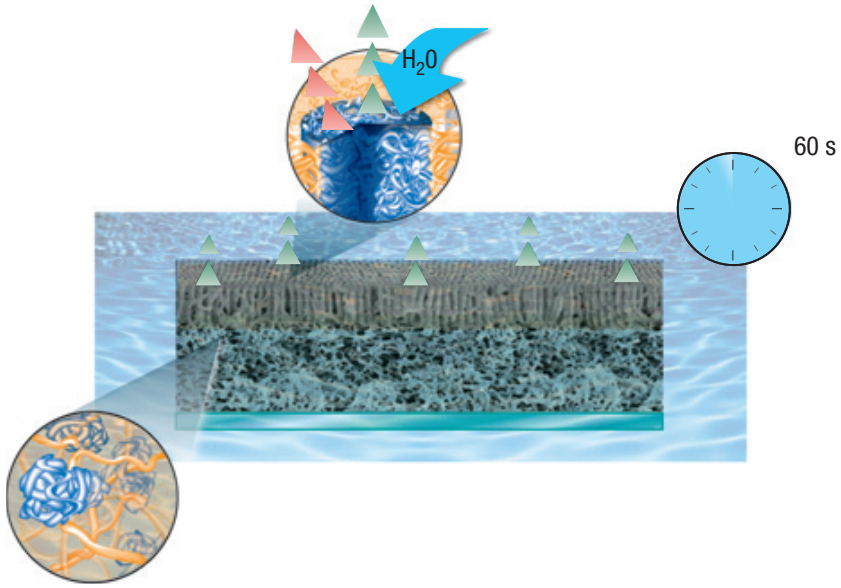

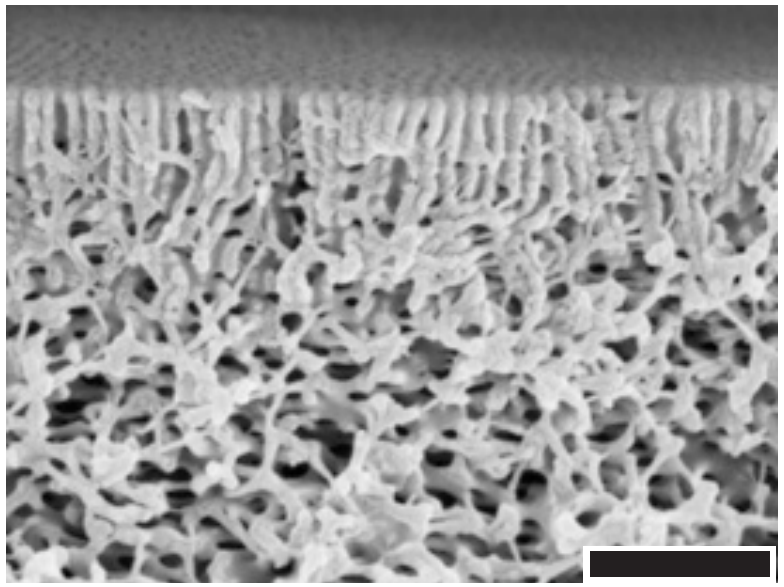

Mix two miscible solvents (DMF and THF) with an amphiphilic di-block co-polymer (PEO-poly vinyl pyridine) one of whose components is soluble only in DMF. Evaporating off the THF changes the ”goodness” of the solvent. Then immerse in water.
K.-V. Peinemann, V. Abetz, P. F. Simon, *Nature Materials* (2007)

Ionomer Membranes: Selective charge transport

NAFION

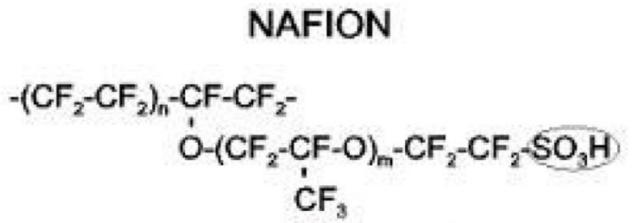

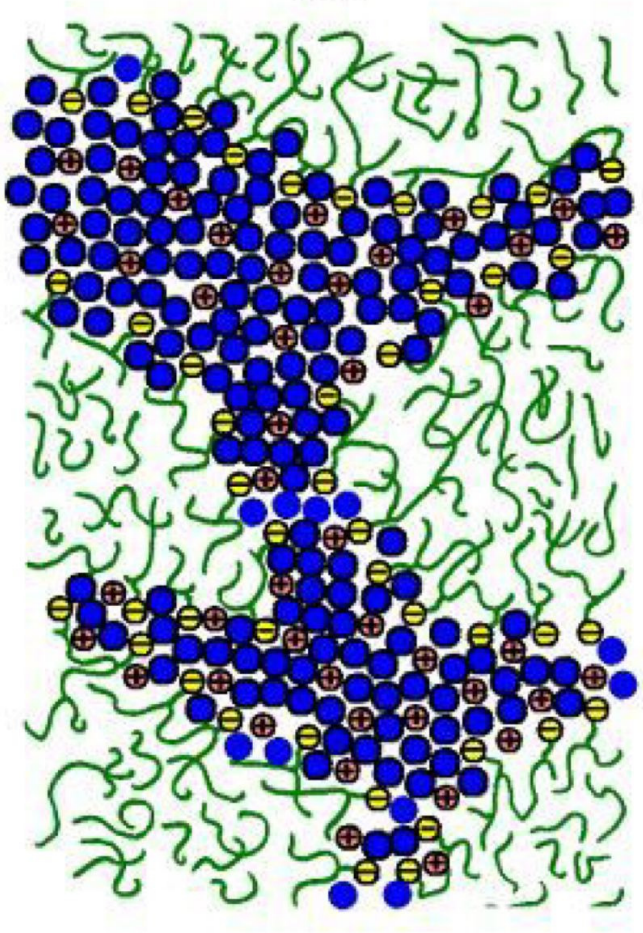

Ionomer Membranes: Incorporation of Solvation Energy

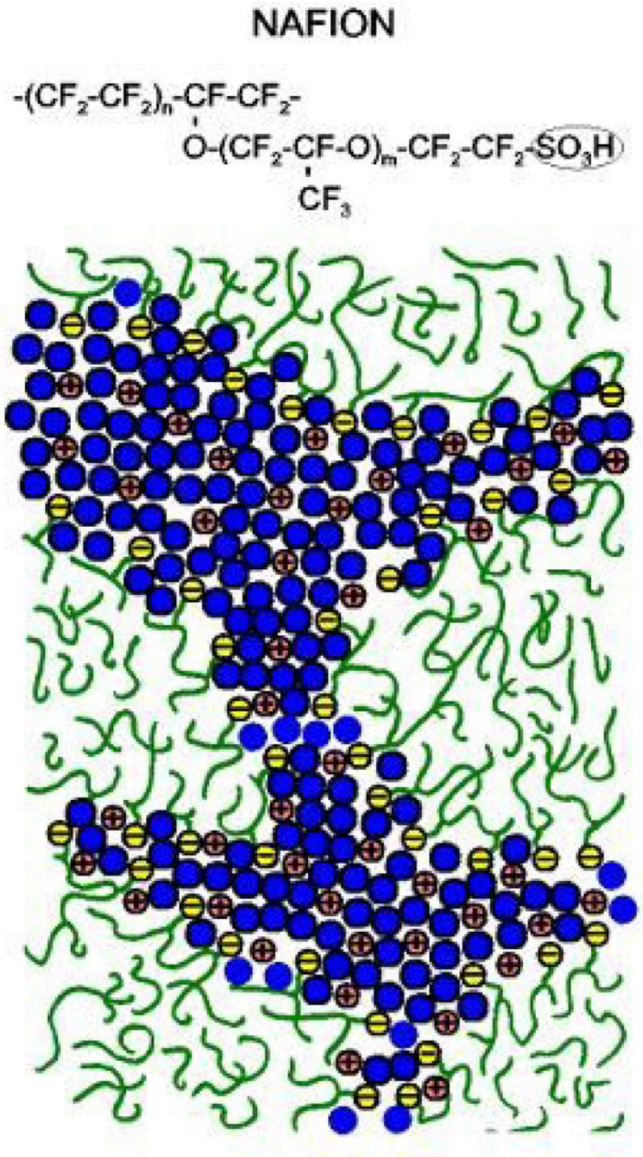

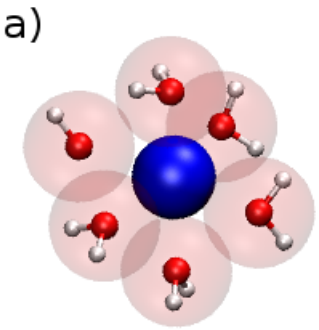

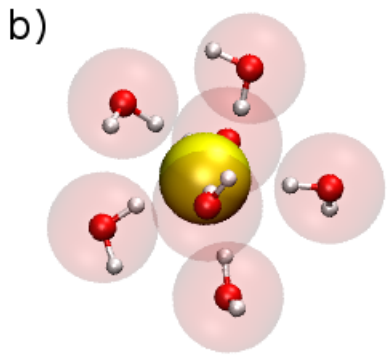

Na^+

F^-

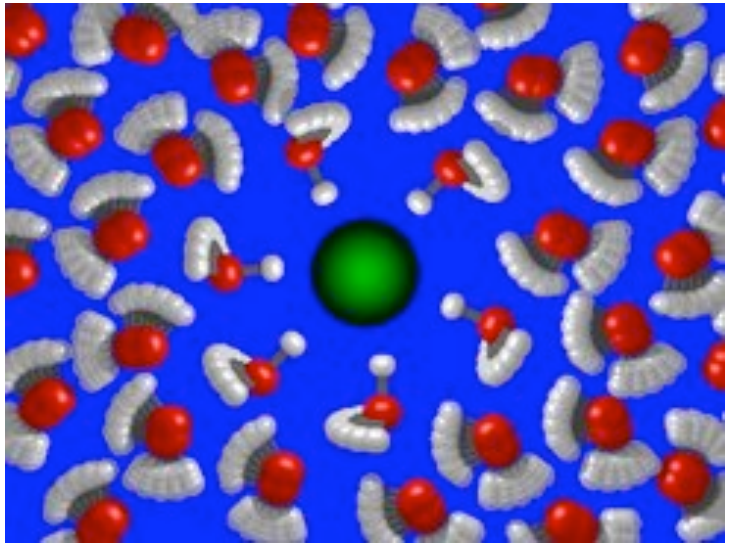

Ionomer Membranes: Incorporation of Solvation Energy

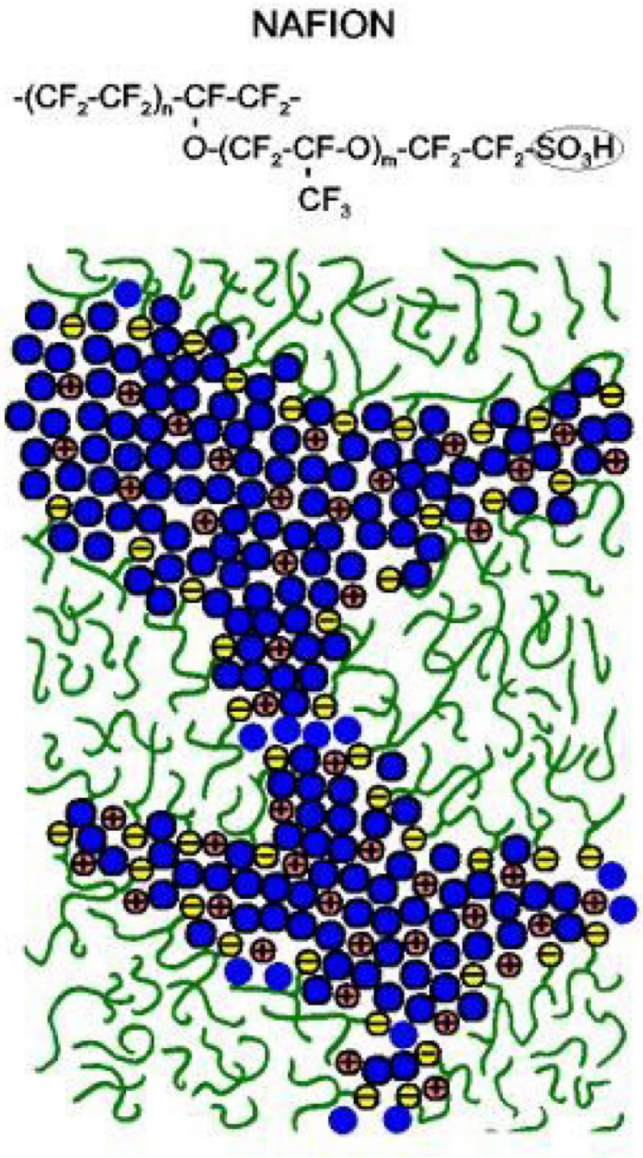

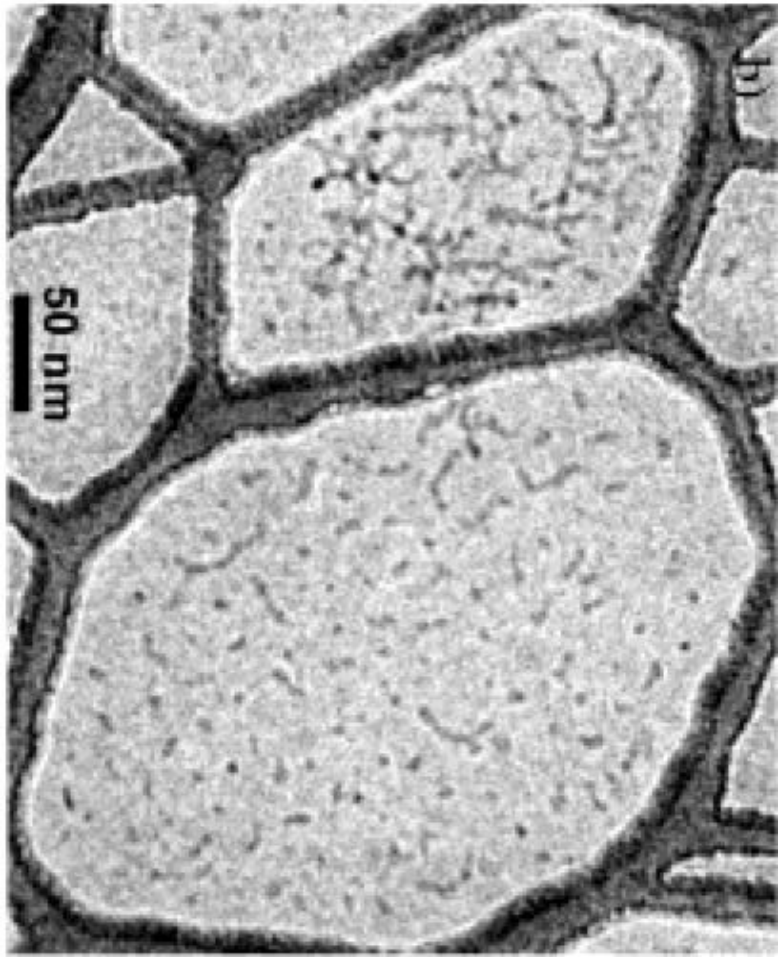

Diat 2004 *Macro.* TEM of Cs^{+}-Nafion

Salt Molarity and Solvation

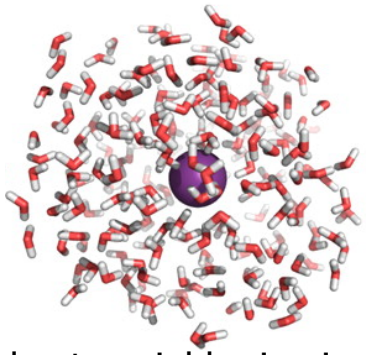

Field due to neighboring ions negligible

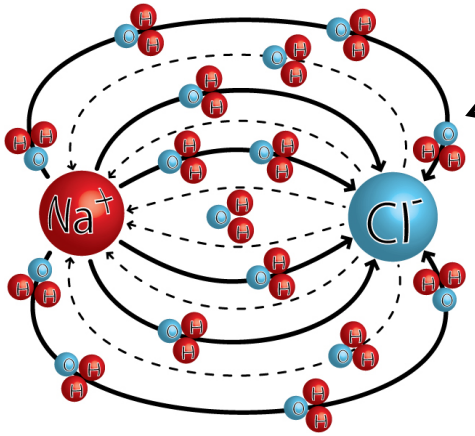

Field due to neighboring ions not negligible
Water screening important

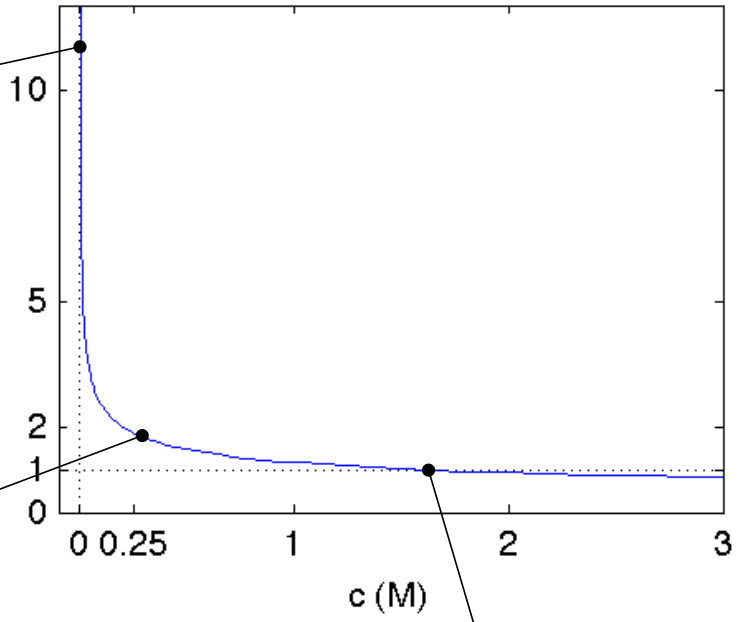

1 nm between ions
Fitting 1-2 water molecules

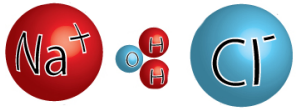

Ionic field dominant
Water screening negligible

Formulation of Solvation Energy

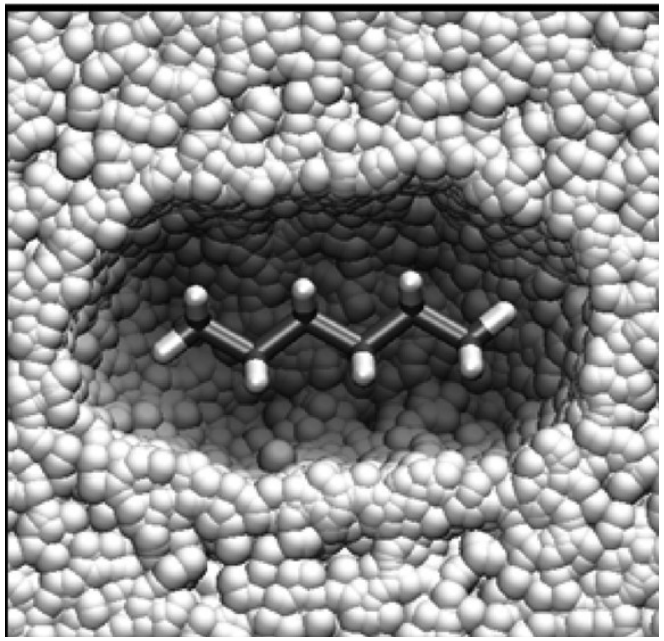

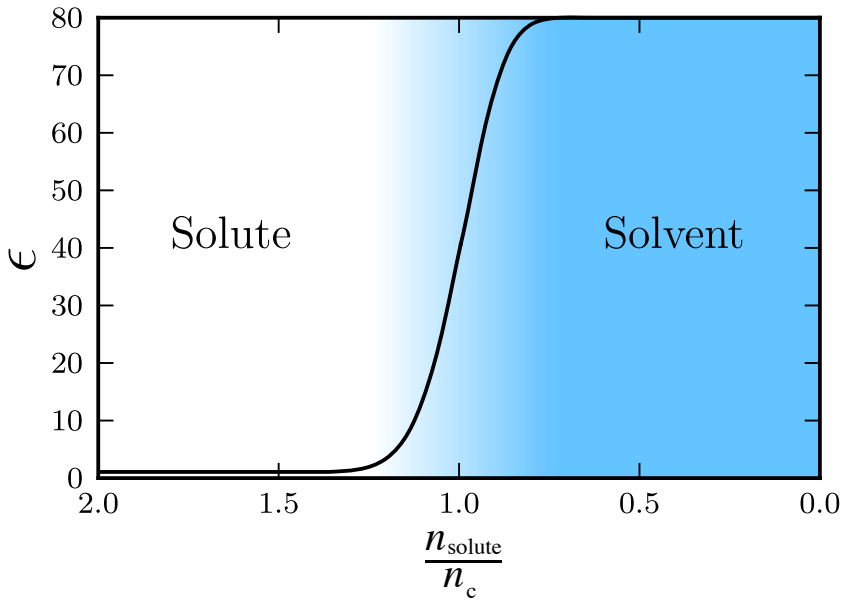

K. Mathew, R. Hennig et al, *J. Chem. Phys.*

Andreussi et al take the dielectic, $\varepsilon = \varepsilon(n_{\text{solute}})$, to be a function of the solute electronic density, with electrostatic energy

$$E^{\text{el}} = \int \varepsilon(n_{\text{solute}}) |\nabla \phi|^2 \, dx,$$

and develop a free energy by adding "quantum surface" and "quantum volume"

$$\Delta G^{\text{sol}} = \Delta G^{\text{el}} + \eta_1 S + \eta_2 V.$$

Andreussi, Dabo, Marzari, *J. Chem. Phys.* **136** (2012)

Direct Quote

"As for the remaining contributions to the solvation free energy, we have decided to treat them in a simplified way, their explicit modeling being the subject of future developments. In particular, similar to other models of solvation, the thermal motion contribution has been neglected, *while we express the sum of dispersion and repulsion free energies as a term linearly proportional to the quantum surface and the quantum volume of the molecular cavity*."

Andreussi, Dabo, Marzari, *JCP* **136** (2012).

Szostak: Primitive cell membranes

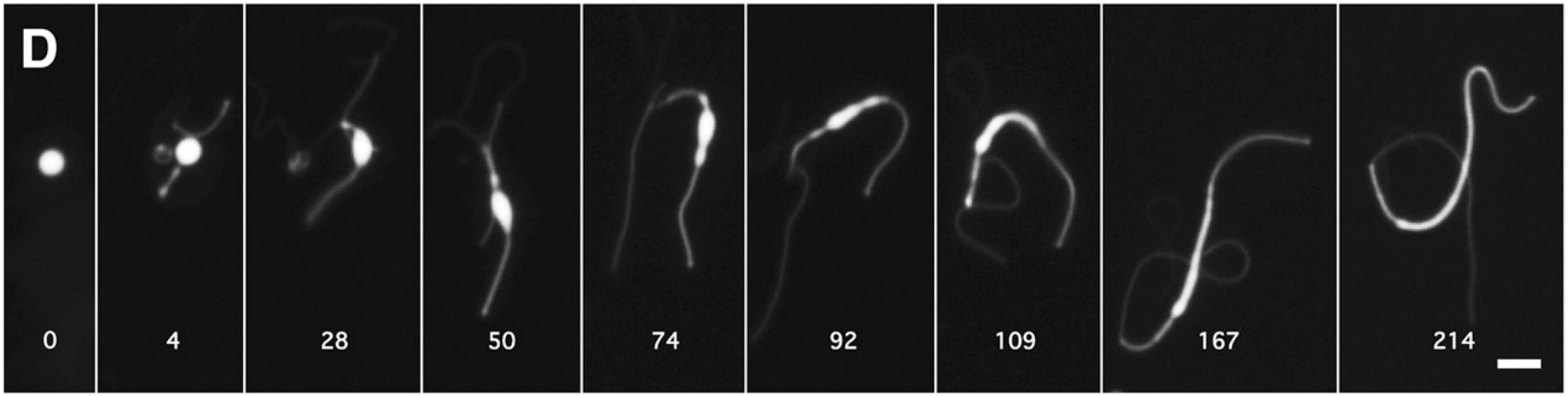

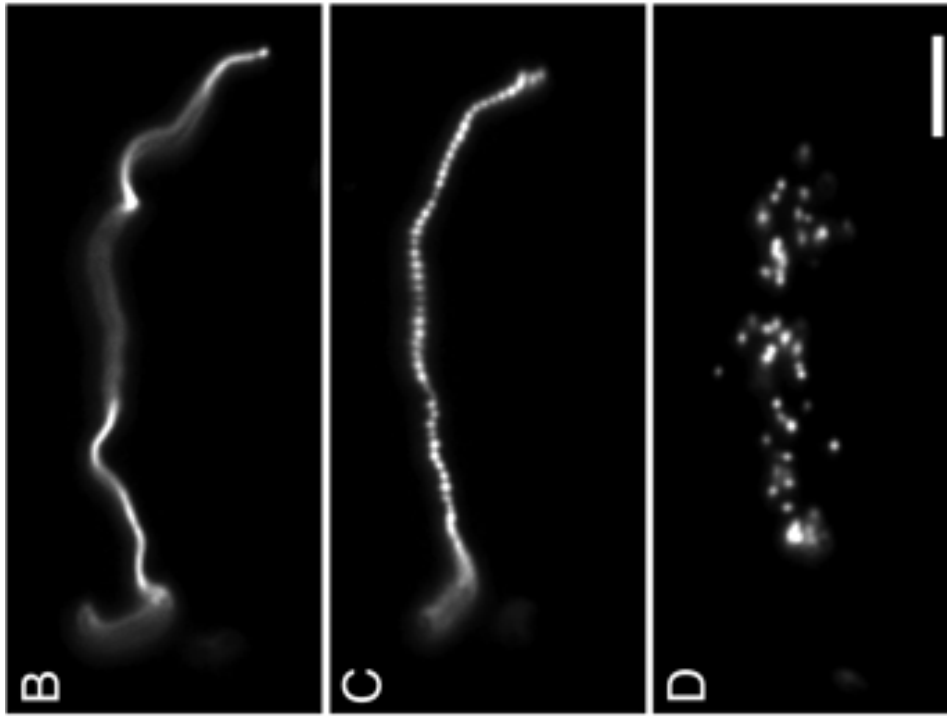

PNAS 2011/2012: primitive membranes had no phospholipids. (top) Mix 10% phospholipid membrane with pure oleate vesicles. (bottom) Radical mediated/photo-induced oxidation of thiols to disulfides induces pearling.

Pearling in amphiphilic di-block blends

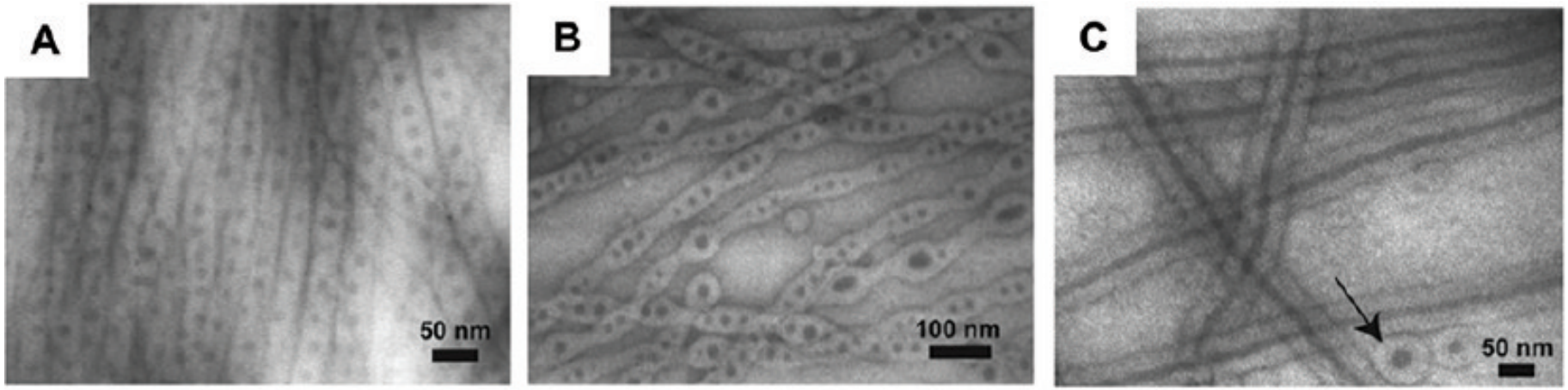

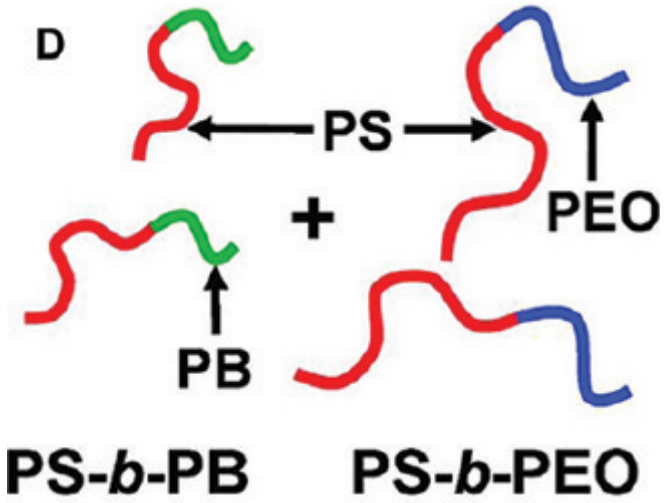

Changes in PS-PB and PS-PEO volume fractions (A) 80:20, (B) 70:30, (C) 60:40, drive pearling bifurcations in the internally separated phase. Hayward et al *Macromolecules* (2008)

Cahn-Hilliard Expansion

Fix $\Omega \subset \mathrm{R}^3$, let $u \in H^1(\Omega)$ denote the volume fraction of one component of a binary mixture. Cahn and Hilliard (1958) expanded the free energy $f(u, \epsilon\nabla u, \epsilon^2\Delta u)$

$$\mathcal{E}(u) = \int_\Omega \frac{\epsilon^2}{2}|\nabla u|^2 + W(u)\, dx.$$

For amphiphilic mixtures: Tuebner & Strey (1987) Gompper & Schick (1990) added higher derivatives

$$\mathcal{F}(u) := \int_\Omega f(u,0,0) + \epsilon^2 A(u)|\nabla u|^2 + \epsilon^2 B(u)\Delta u + \epsilon^4 \overbrace{C(u)}^{\geq 0} (\Delta u)^2\, dx.$$

Complete the square

$$\mathcal{F}(u) := \int_\Omega C(u)\Big(\epsilon^2\Delta u - \overbrace{\boxed{\frac{\overline{A} - B}{2C}}}^{W'(u)}\Big)^2 + \overbrace{\boxed{f(u) - \frac{(\overline{A} - B)^2}{C(u)}}}^{P(u)}\, dx.$$

When $P \ll 1$, then the energy is very degenerate, very special.

$$\boxed{\mathcal{F}(u) = \int_\Omega \frac{1}{2}\left(\epsilon^2\Delta u - W'(u)\right)^2 - \epsilon^2\left(\eta_1\frac{\epsilon^2}{2}|\nabla u|^2 + \eta_2 W(u)\right)\, dx.}$$

Functionalization parameters $\eta_1 > 0$ and $\eta_2 \in \mathbb{R}$.

Functionalized Cahn-Hilliard Energy

An unfolding of the De Giorgi energy:

$$\mathcal{F}_{\mathrm{CH}}(u) = \int_{\Omega} \frac{1}{2}\left(\epsilon^2 \Delta u - W'(u;\tau)\right)^2 - \boxed{\epsilon^p\left(\frac{\epsilon^2\eta_1}{2}|\nabla u|^2 + \overbrace{\Pi(u)}^{\eta_2 W(u)}\right)} \, \mathrm{dx}.$$

$p = 1$ Strong Functionalization
$p = 2$ Weak Functionalization

The parameters: η_1 strength of hydrophilic portion of amphiphilic component. Pressure jump $\Pi(u)$ between phases – parameterize by η_2. Interfacial structure parameterized by "tilt" parameter τ.

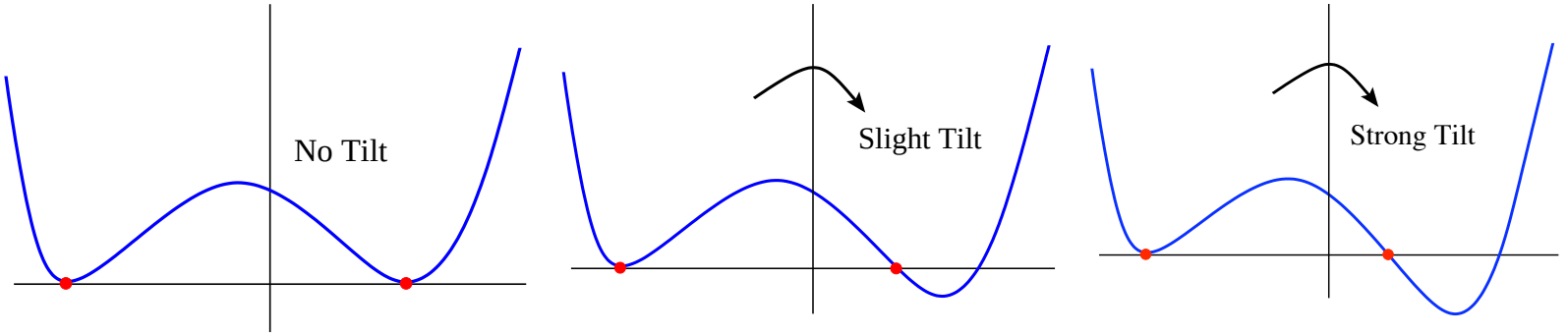

Bi-Layers: Co-Dimension One

Near a hypersurface $\Gamma \subset \mathbb{R}^n$, the Laplacian becomes

$$\epsilon^2 \Delta = \partial_z^2 + \epsilon H \partial_z + \epsilon^2 \Delta_s$$

where H is the mean curvature of the interface, and Δ_s is a surface diffusion.

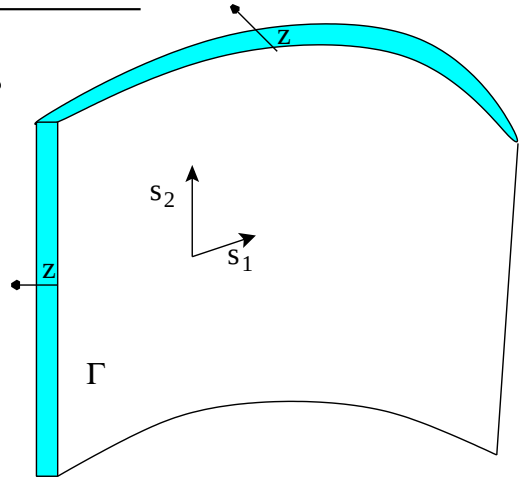

The variational derivative can be made small

$$\epsilon^2 \Delta \phi_b - W'(\phi_b) = O(\epsilon),$$

if co-dim 1 inner structure, ϕ_b, solves

$$\partial_z^2 \phi_b - W'(\phi_b) = 0.$$

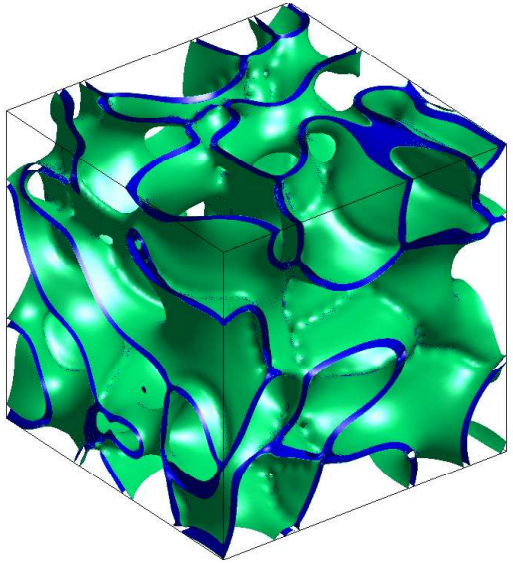

The residual of the squared-variational term is

$$\left(\epsilon^2 \Delta \phi_b - W'(\phi_b)\right)^2 =$$

$$\left(\boxed{\partial_z^2 \phi_b - W'(\phi_b)} + \epsilon H \phi_b' + \ldots\right)^2,$$

$$= \epsilon^2 \left(\phi_b(z)'\right)^2 H(s)^2.$$

Pores: Co-Dimension Two

Fix $\Gamma \subset \mathbb{R}^3$, a cylindrical geometry leads to (R, θ, s) variables and the decomposition

$$\epsilon^2 \Delta = \Delta_R - \begin{pmatrix} \kappa_1 \\ \kappa_2 \end{pmatrix} \cdot \begin{pmatrix} \partial_{z_1} \\ \partial_{z_2} \end{pmatrix} + \epsilon^2 D_s^2.$$

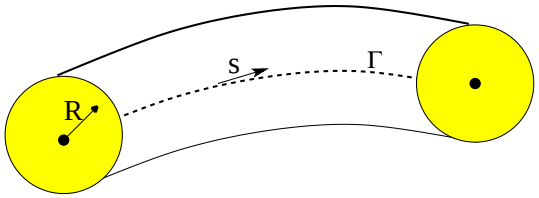

With angular symmetry, the co-dim 2 inner structure satisfies

$$\partial_R^2 \phi_2 + \frac{1}{R} \partial_R \phi_p = W'(\phi_p),$$

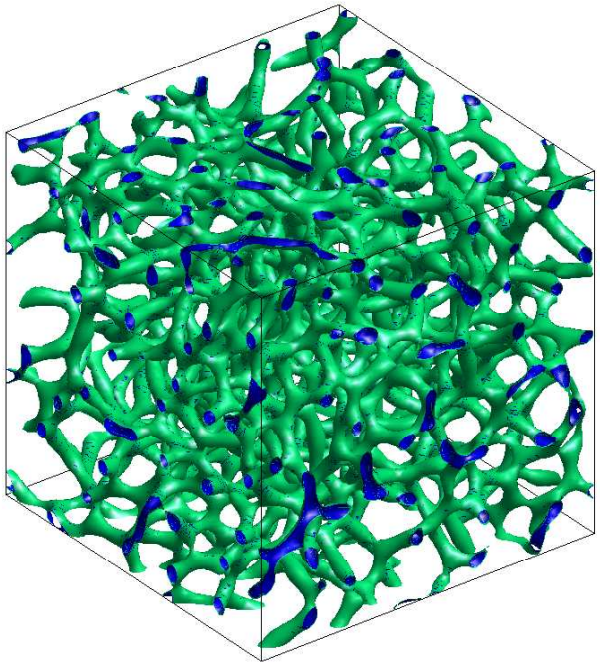

where (R, θ) are polar versions of (z_1, z_2). The squared-variational remainder is

$$\left(\epsilon^2 \Delta \phi_p - W'(\phi_p)\right)^2 = \epsilon^2 \left(\phi_p'\right)^2 |\kappa|^2.$$

The Well Tilt Parameter τ

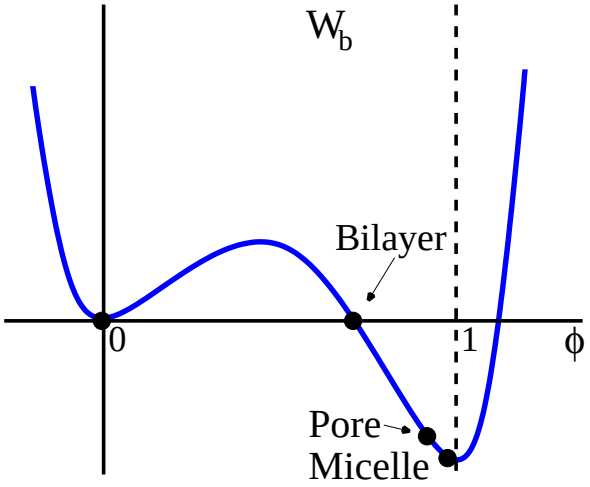

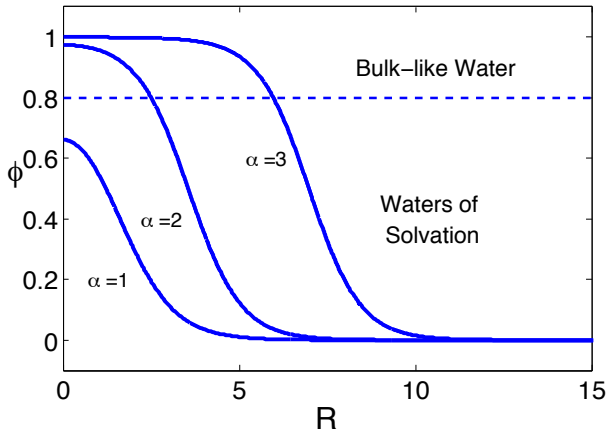

Well tilt, τ differentiates the self-energy of the solvent and polymer phases.

$$\partial_R^2 \phi_\alpha + \frac{\alpha - 1}{R} \partial_R \phi_\alpha = W'(\phi_\alpha; \tau).$$

The liquid-phase self energy is reflected by its pressure

$$P = P_l + P_{\text{osm}}, \qquad P_{\text{osm}} = RT\rho_+ \approx 80 - 100 \frac{\text{J}}{\text{cm}^3}.$$

The balance between the liquid pressure and bulk modulus of polymer phase tunes the pore radius. This is encoded in a constitutive relation for the well-tilt:

$$\tau = \tau(P).$$

The Well Tilt Parameter τ

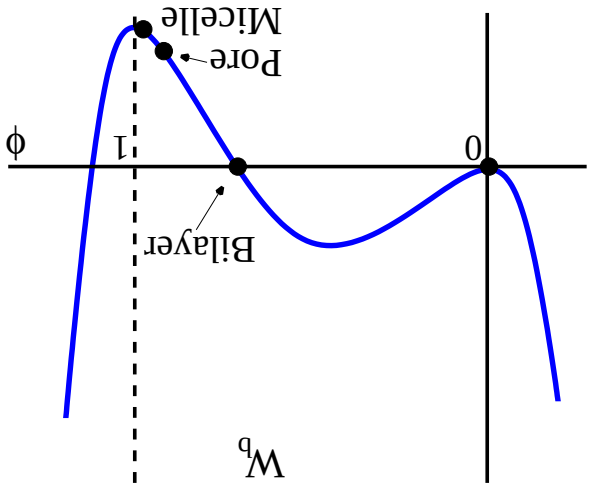

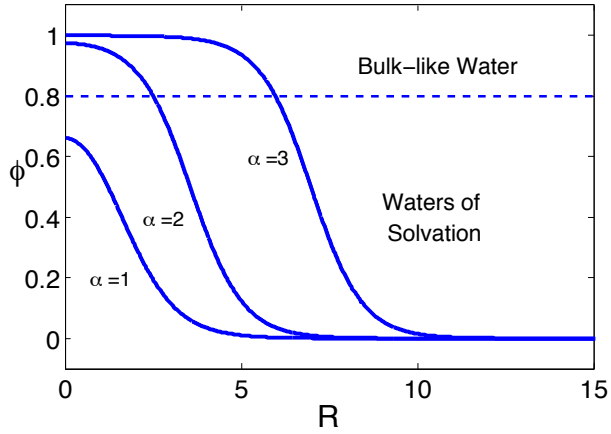

Well tilt, τ differentiates the self-energy of the solvent and polymer phases.

$$\partial_R^2 \phi_\alpha + \frac{\alpha - 1}{R} \partial_R \phi_\alpha = W'(\phi_\alpha; \tau).$$

The liquid-phase self energy is reflected by its pressure

$$P = P_l + P_{\text{osm}}, \qquad P_{\text{osm}} = RT\rho_+ \approx 80 - 100 \frac{\text{J}}{\text{cm}^3}.$$

The balance between the liquid pressure and bulk modulus of polymer phase tunes the pore radius. This is encoded in a constitutive relation for the well-tilt:

$$\tau = \tau(P).$$

Unfolding of the De Giorgi Energy

$$\mathcal{F}_{\mathrm{CH}}(u) = \int_\Omega \frac{1}{2}\left(\epsilon^2 \Delta u - W'(u)\right)^2 - \epsilon^p \left(\frac{\eta_1}{2}\epsilon^2 |\nabla u|^2 + \eta_2 W(u)\right) dx.$$

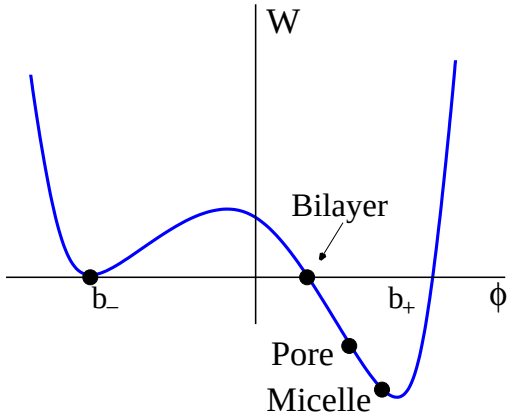

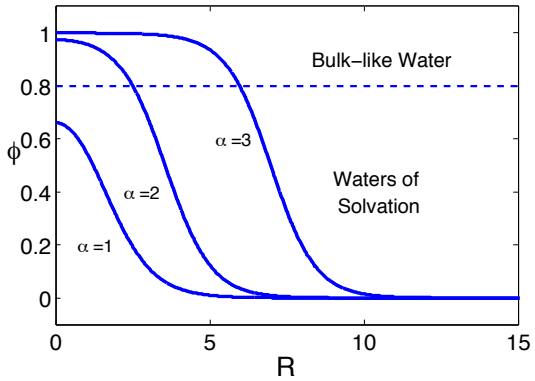

Co-dim 1	$\partial_z^2 \phi_b = W'(\phi_b)$	$\int_\Omega W(\phi_b)\, dx > 0$
Co-dim 2	$\frac{1}{R}\partial_R(R\partial_R)\phi_p = W'(\phi_p)$	$\int_\Omega W(\phi_p)\, dx = 0$
Co-dim 3	$\frac{1}{R^2}\partial_R(R^2\partial_R)\phi_m = W'(\phi_m)$	$\int_\Omega W(\phi_m)\, dx < 0.$

Impact of Volume Term

$$\mathcal{F}_{\mathrm{CH}}(u) = \int_{\Omega} \frac{1}{2}\left(\epsilon^2 \Delta u - W'(u)\right)^2 - \epsilon^p \left(\frac{\eta_1}{2}\epsilon^2 |\nabla u|^2 + \eta_2 W(u)\right) dx.$$

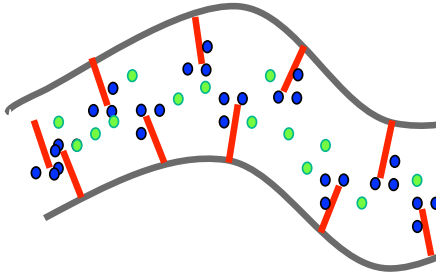

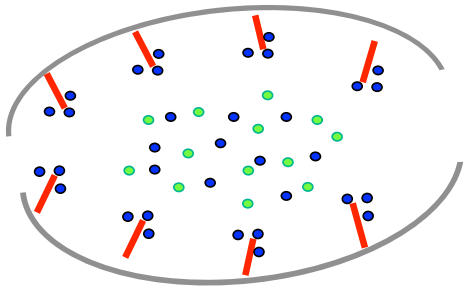

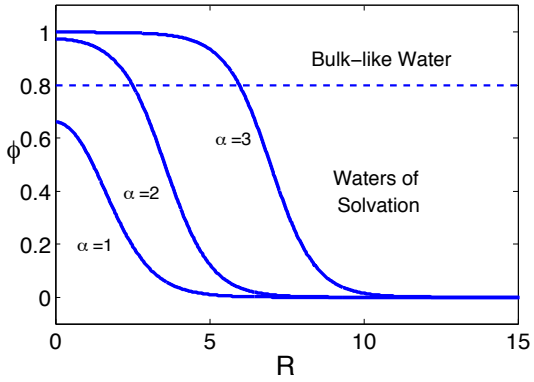

For pores in Nafion, the parameter η_2 could express the counter-ion's (protons) preference for bulk-like water verses waters of solvation.

Key Prediction: A preference for bulk-like water selects pores over bilayers and selects micelles over pores.

Small Sample of Parameter Space $\tau = -0.4$, $\epsilon = 0.03$

$$u_t = \Delta \frac{\delta \mathcal{F}_{\mathrm{CH}}}{\delta u} \quad \Longrightarrow \quad \frac{d}{dt}\mathcal{F}_{\mathrm{CH}}(u) \leq 0$$

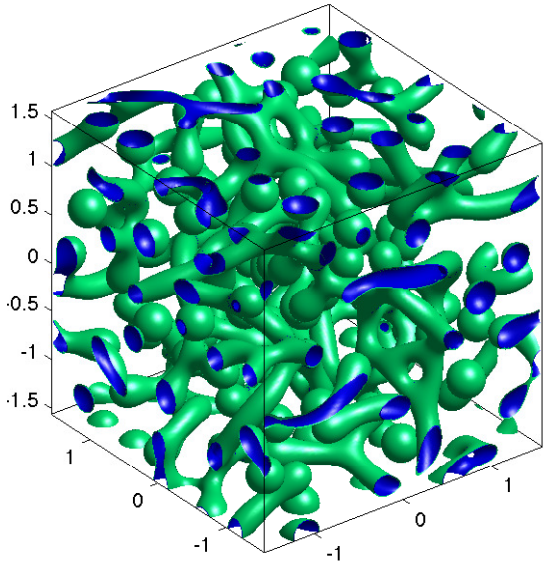

$\eta_2 = -2$
Micelles - Pores
Co-dim 2 & 3

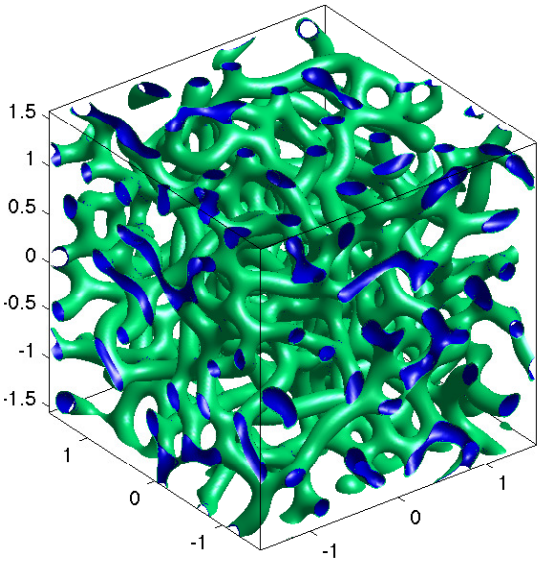

$\eta_2 = 1$
Pore Network
Co-dim 2

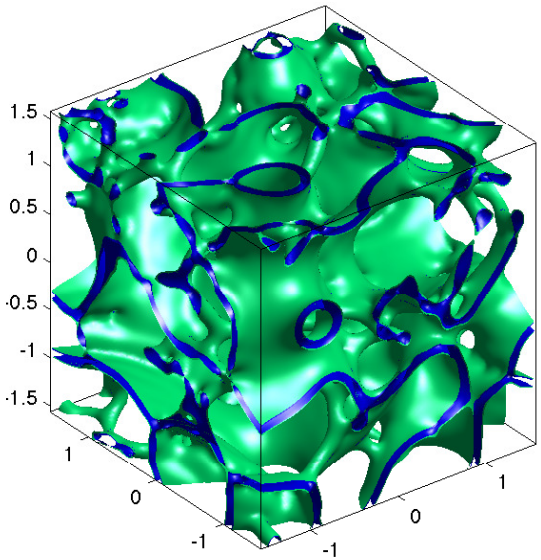

$\eta_2 = 3$
Bilayers
Co-dim 1

Identical, randomly ± 1 initial data. Co-dimension = choice of inner structure.

Experimental Morphology

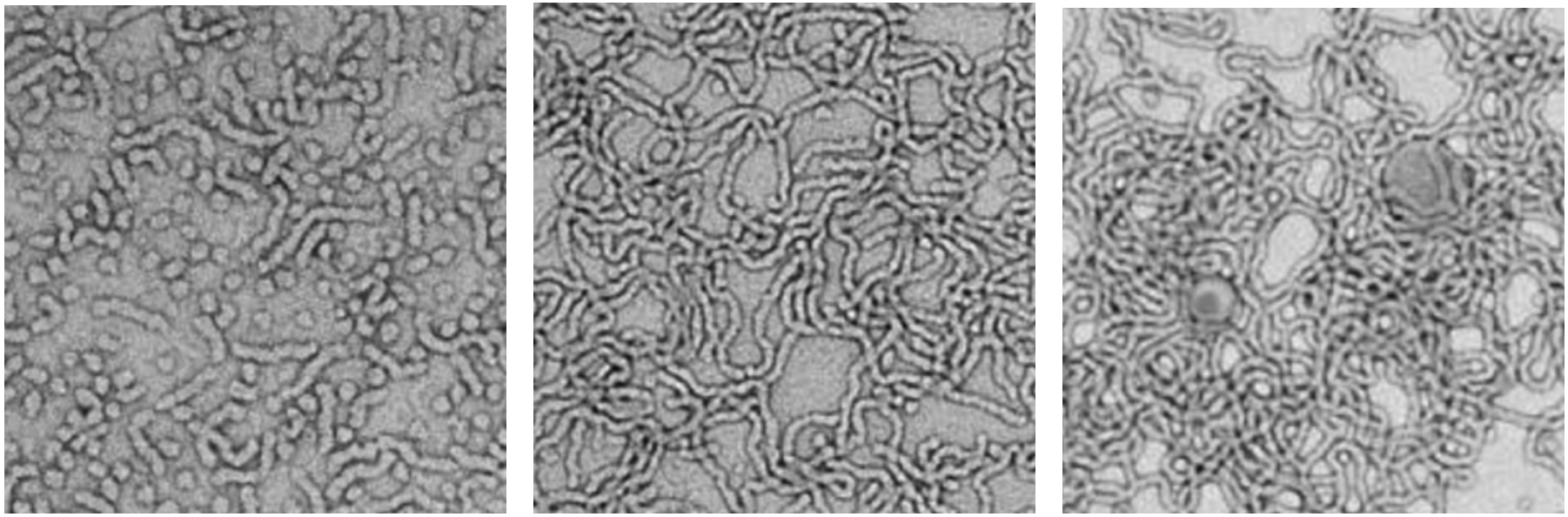

Blends of amphiphilic diblock copolymers with fixed lengths of hydrophilic block and differing lengths of hydrophobic chain. The diblocks with the longest hydrophobic chains from coexisting micelle/worm structures, while decreasing hydrophobic chain length leads to worm only, and coexisting worm/bilayer (hollow) vesicles.
L. Ratcliffe, A. Ryan, and S. Armes, *Macromolecules* **46** (2013).

Bifurcation Diagram

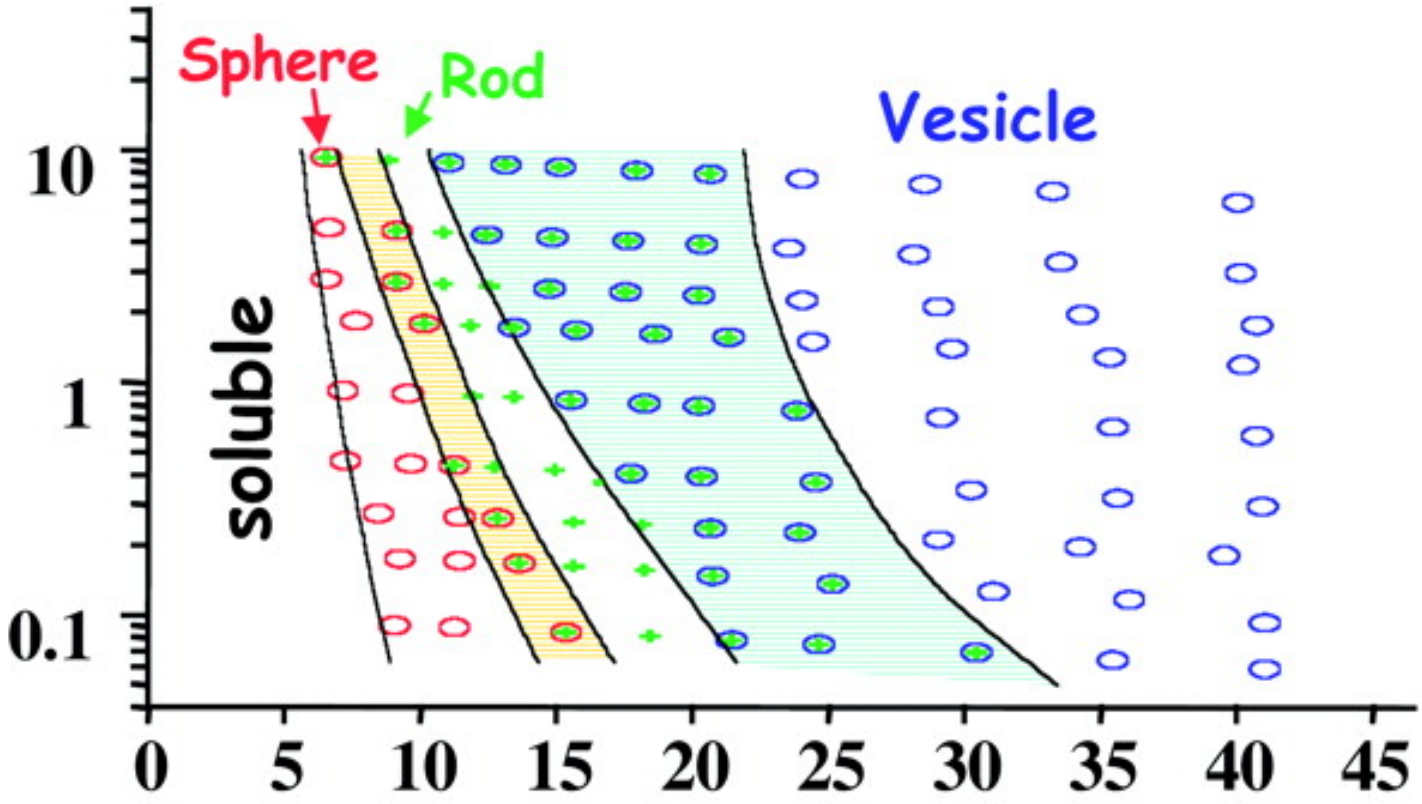

Bifurcation diagram for amphiphilic copolymers as function of weight percent of copolymer (vertical log axis) and water volume fraction within water-dioxane solvent blend (horizontal axis). Increasing water fraction drives bifurcations from micelle (sphere) to pore (rod) to bilayer (vesicle), shaded regions indicate pearling and co-existence, from D. Dicher and A. Eisenberg, *Science* **297** (2002).

Merging of Dumb-bell Structures into Pore Network

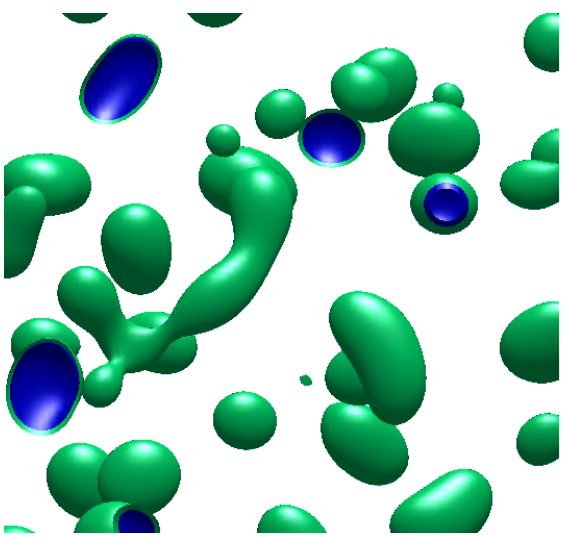

(a)

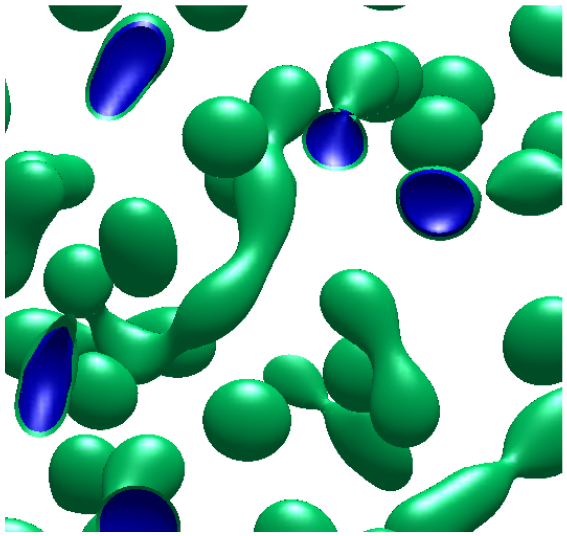

(b)

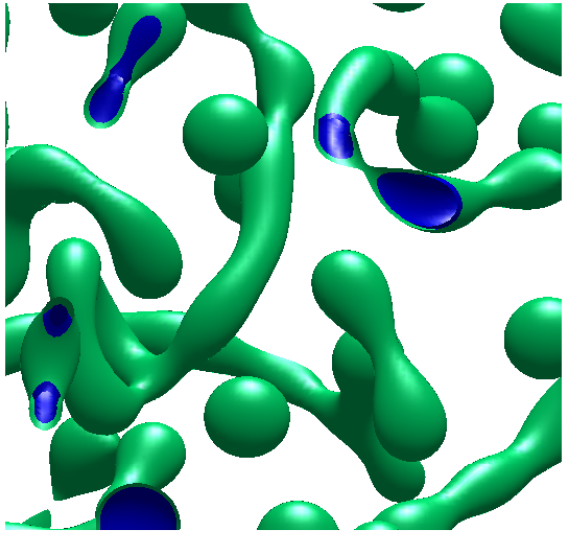

(c)

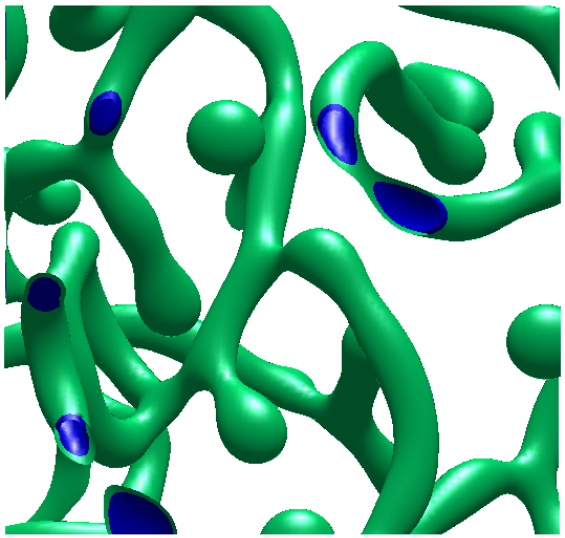

(a) Random initial data coarsens into micelles,
(b) over-sized micelles are unstable and grow into dumb-bells,
(c-d) dumb-bells elongate, merge and form a pore network.

Nafion and SAXS Data

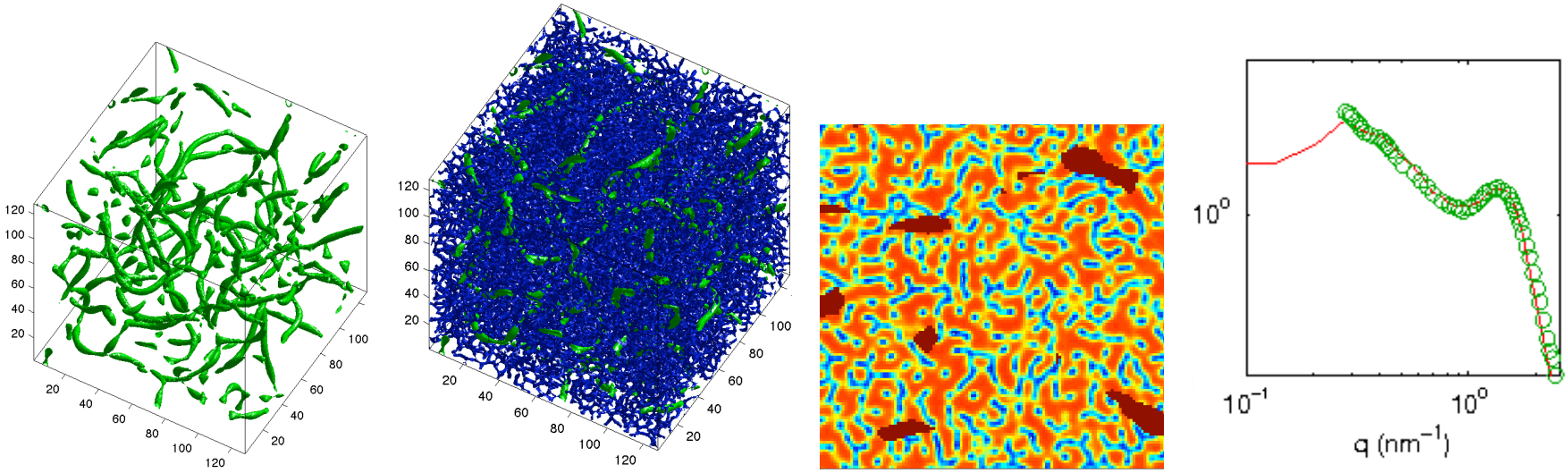

(A) (B) (C) (D)

(A) Crystalline network calculated has smaller (negative) η_i .

(B) The solvent network (blue) has larger (positive) values of η_i and non-zero tilt τ.

(C) Cross-section of solvent-crystalline matrix, enlarged for detail.

(D) SAXS data: Log of scattering intensity verses Log of scattering parameter q, in $\mathbf{nm}^{-}$,[1]for the composite network (red line) and experimental data of hydrated Nafion, Rubidat-2002 (circles).

Gavish, Jones, Xu, Christlieb, Promislow *Polymers* (2012).

Dehydrating Nafion

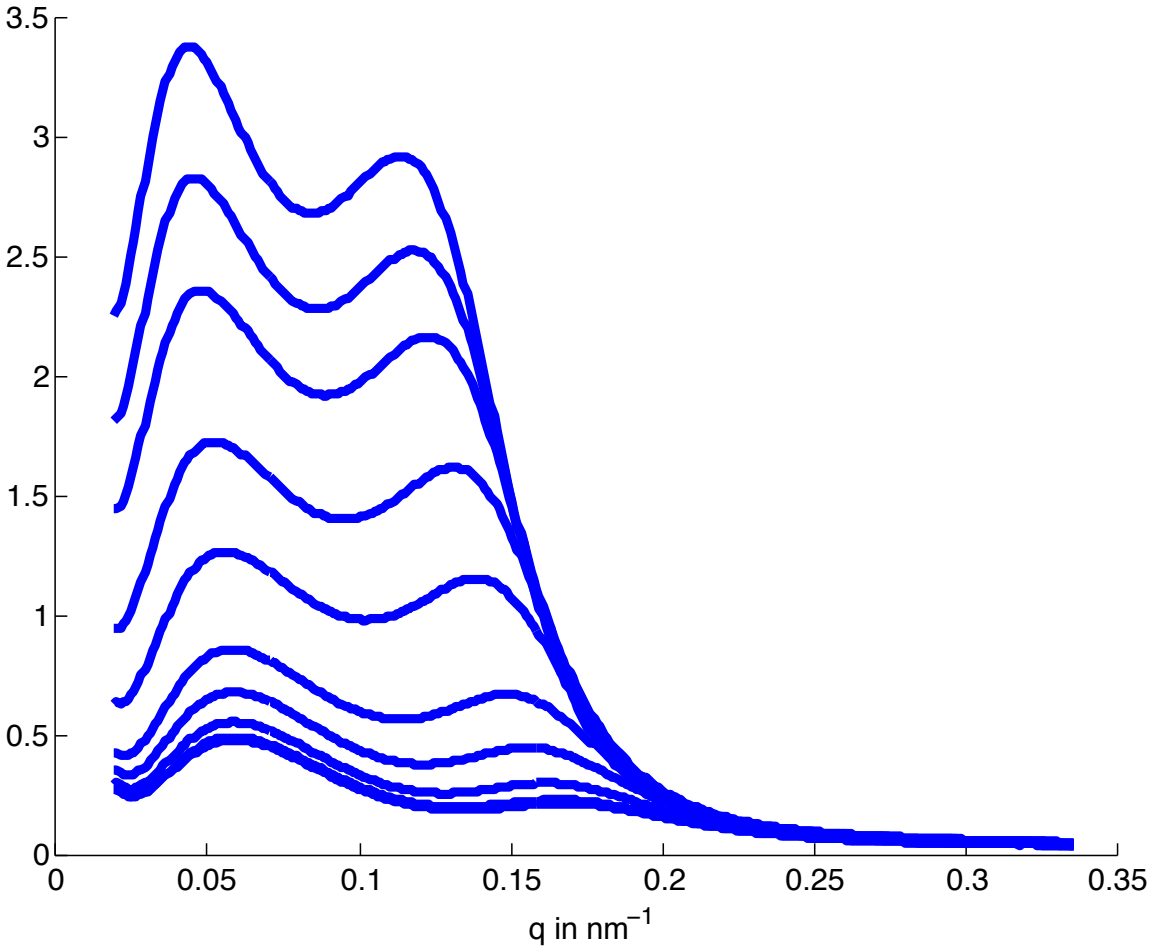

SAXS data of Nafion in a dehydrating environment, from 3 to 20 minutes. Courtesy of Robert Moore, Virginia Tech.

Spectra of Functionalized Bilayers

$$u_b(x) = \phi_b(z) + \epsilon^2(\gamma_2 + H^2(s)\phi_{2,\mathrm{loc}}(z)) + O(\epsilon^3)$$

Stability of bilayers determined by the eigenvalues of the second variation

$$\mathbb{L} := \frac{\delta^2 \mathcal{F}}{\delta u^2}(u_b),$$
$$= (\partial_z^2 - W''(\phi_b) + \epsilon^2 \Delta_s)^2 + O(\epsilon),$$

whose eigenfunctions separate to $O(\epsilon)$,

$$\Psi_{j,n} = \psi_j(z)\Theta_n(s) + O(\epsilon).$$

Instability can come from pearling (ground-state ψ_0 with $\lambda_0 > 0$) or meander eigenvalues ($\psi_1 = \phi_b'$ with $\lambda_1 = 0$).

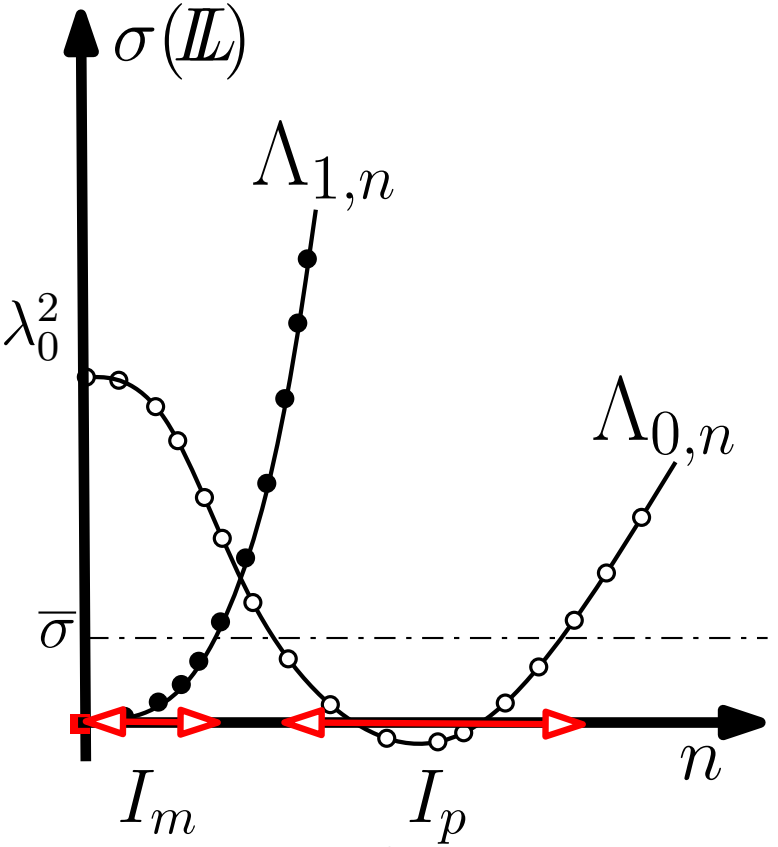

$$\Lambda_{0,n} = (\lambda_0 - \epsilon^2\beta_n)^2 + \epsilon[\lambda_0(\eta_1 - \eta_2) - \gamma_2 S] + O(\epsilon^2).$$

The sign of S determines if pearling absorps or liberates solvent, connecting background level γ to the pearling bifurcation.

Numerical Validation: Initial data bilayer is too wide.

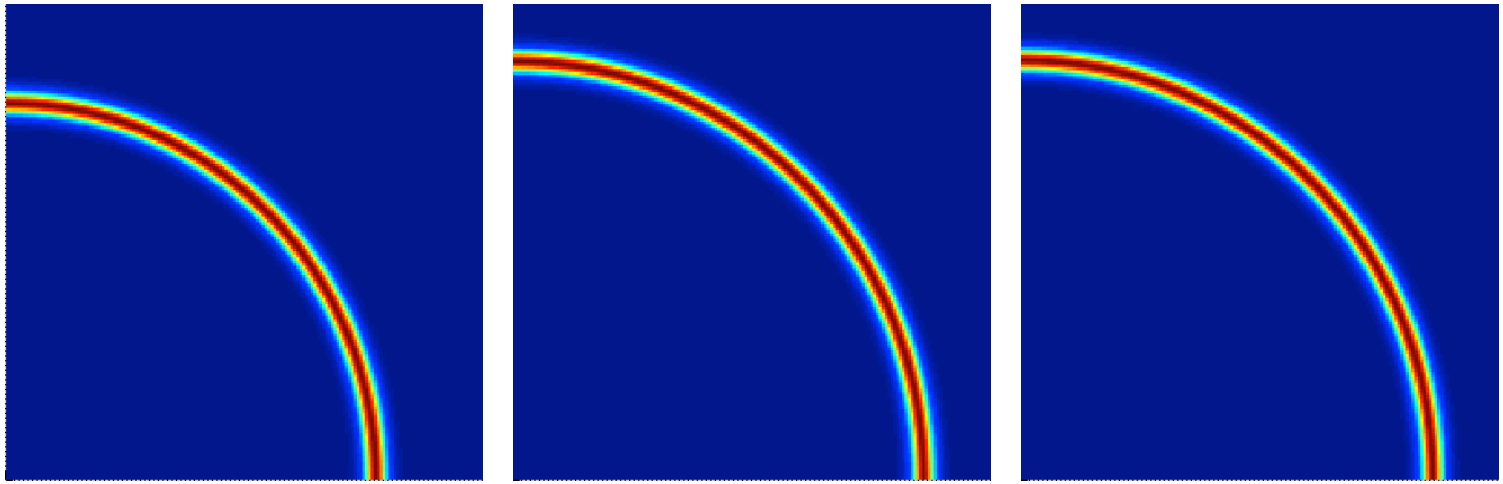

Images for $\epsilon = 0.1$, $\eta_1 = 1$, and $\eta_2 = 2$ at times $t = 0$, $t = 857$, and $t = 3000$. No pearling, convergence to equilibrium on the $O(\epsilon^{-3})$ time-scale.

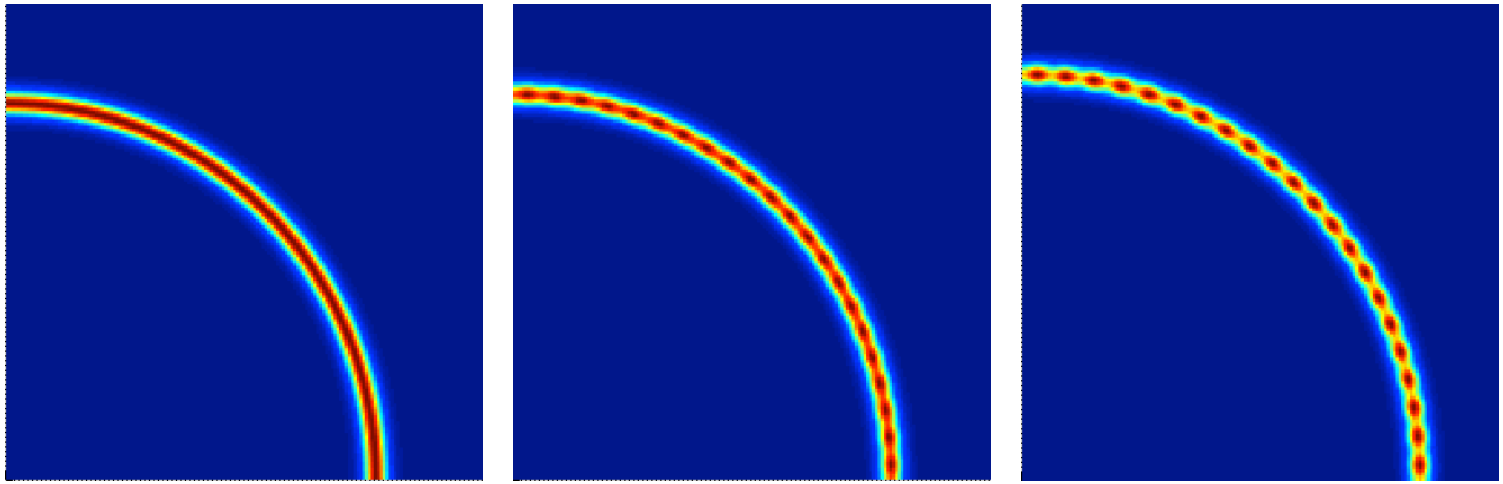

(Szostak) $\epsilon = 0.1$, $\eta_1 = \eta_2 = 2$ at times $t = 0$, $t = 114$, and $t = 804$.

Pearling Bifurcation in Pores

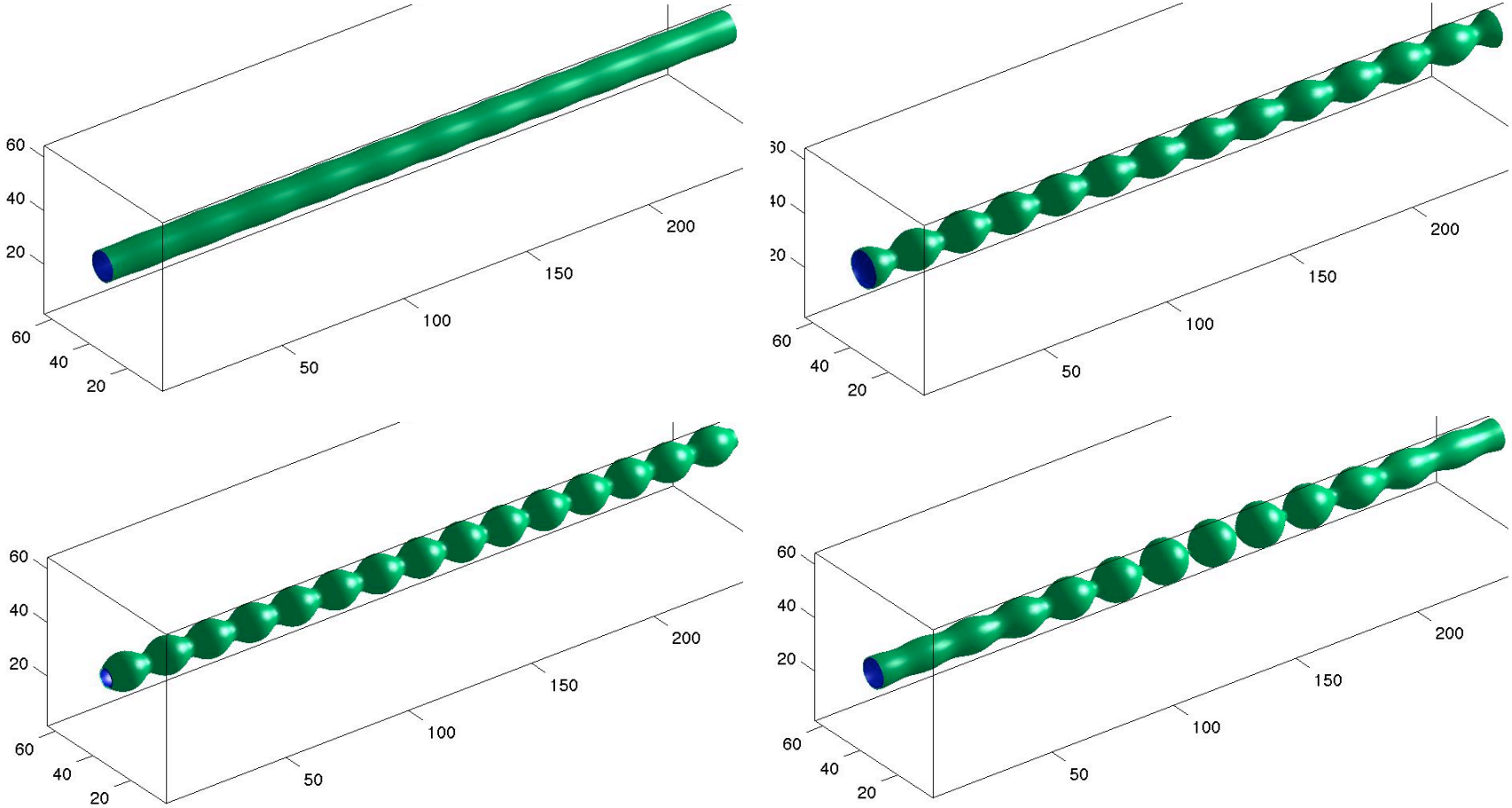

Equilibria after evolution from a cylindrically symmetric, perturbed pore for $\eta_1 = 5$ and $\eta_2 = -4, -6, -8, -10$ respectively.

Geometric Evolution of Bilayers, $\mathcal{G} = -\Delta$, (Shibin Dai)

$$u_t = -\Delta \frac{\delta \mathcal{F}}{\delta u},$$

At $t_1 = \epsilon t$, for a bilayer Γ we obtain the Mullins-Sekerka flow for μ_1:

$$\begin{aligned} \Delta \mu_1 &= 0, && \text{in } \Omega \backslash \Gamma, \\ \mu_1 &= c(t_1) + H\phi_b'(0), && \text{on } \Gamma, \\ [\![\partial_n \mu_1]\!] &= 0 && \text{on } \Gamma, \end{aligned}$$

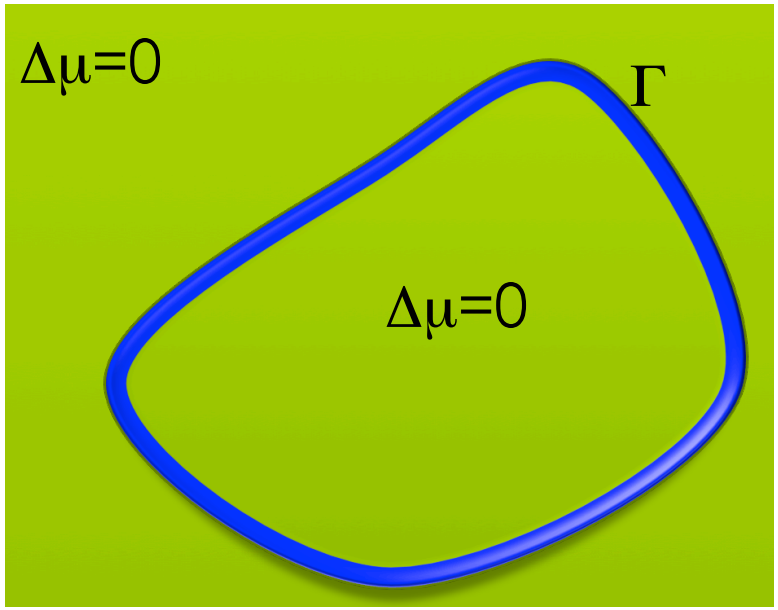

normal velocity $V_b = \partial_n \mu_1^- - \mu_1 H$.

The chemical potential μ_1 is spatially constant, the normal velocity reduces to

$$V_b = -\mu_1 H$$

$$\Longrightarrow \quad \partial_{t_1} H = -\mu_1 \left(\partial_s^2 H + H^3 \right),$$

coupled to the conservation of mass expression

$$\mu_1'(t_1) = -\mu_1(t_1) \int_\Gamma H^2(s)\, ds.$$

The coupled system *prevents* singularity by driving $\mu_1 \to 0$, for $\mu_1(0)$ small enough and $H(0, s)$ not too big.

Competitive Geometric Evolution

At $t_2 = \epsilon^2 t$, the chemical potential is again spatially constant, $\mu_2 = \mu_2(t_2)$,

$$V_b = \frac{\sigma_b}{m_b}\left(\Delta_s + K - \frac{1}{2}H^2 + \frac{\eta_1 + \eta_2}{2} + \lambda_b \mu_2\right) H,$$

For co-dimension two structures in $\mathbb{R}^3$ we derive a similar result for the two-dimensional normal velocity $\vec{\mathbf{V}}_p$ of a space-curve (pore) Γ,

$$\vec{\mathbf{V}}_p = -\frac{\sigma_p}{m_p}\left(\partial_s^2 + \frac{1}{4}|\vec{\kappa}|^2 + \eta_1 + \lambda_p \mu_2\right)\vec{\kappa},$$

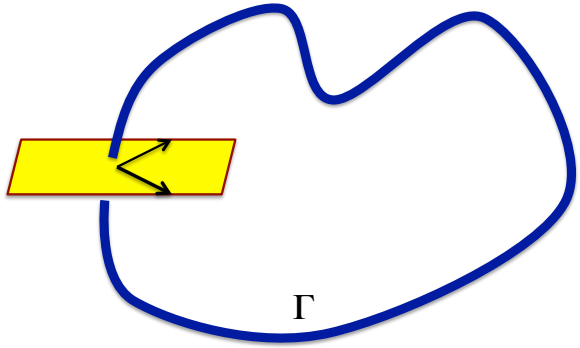

The common value of the chemical potential, μ_2, is fixed by conservation of mass

$$\begin{aligned} 0 &= m_b \frac{d}{dt}|\Gamma_b| + m_p \epsilon \frac{d}{dt}|\Gamma_p|, \\ &= m_b \int_{\Gamma_b} V_b(S) H(S)\, dS - m_p \epsilon \int \vec{\mathbf{V}}_p(s) \cdot \vec{\kappa}(s)\, ds. \end{aligned}$$

– a semi-strong interaction.

Competition and Pearling in Bilayers

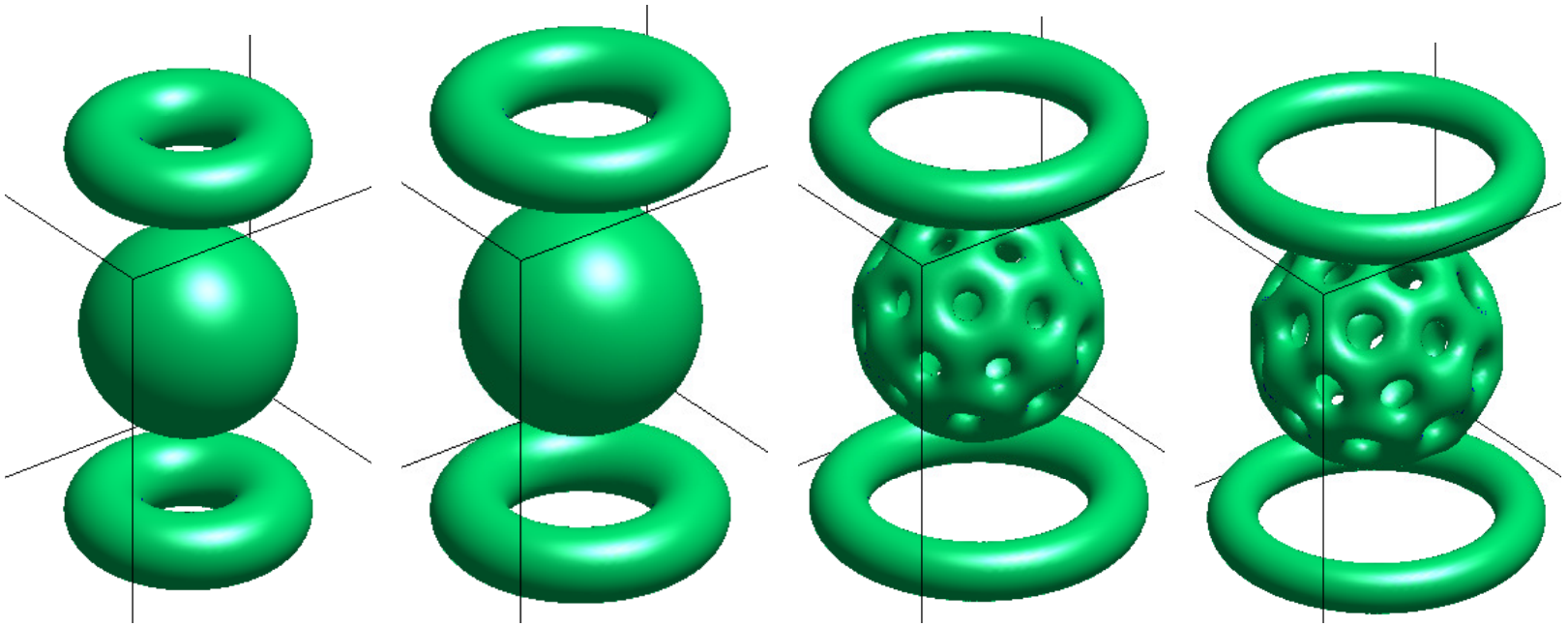

Competition for the amphiphilic phase between spherical bilayer (beach ball) and circular solid pore (hula hoop) as a function of the well-tilt. Well with small tilt prefers bilayers, larger tilt prefers pores and drives bilayers to pearl.

Punctured Vesicle - ETD

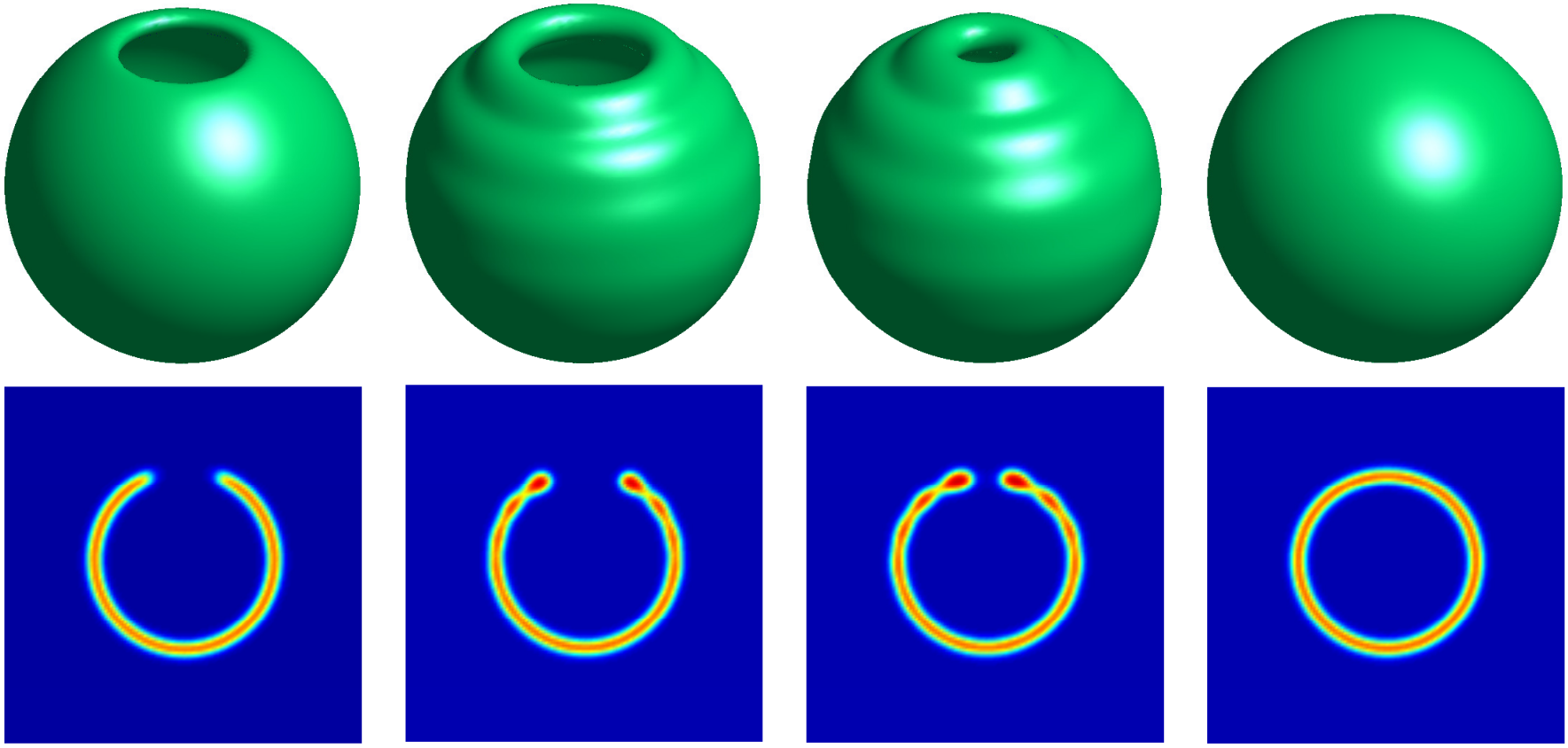

$T = 0$ $T = 0.5$ $T = 10.0$ $T = 15.0$

Time evolution of a punctured Bilayer under ETD. Under convex splitting vesicle failed to close.

Meander induces Endocytosis

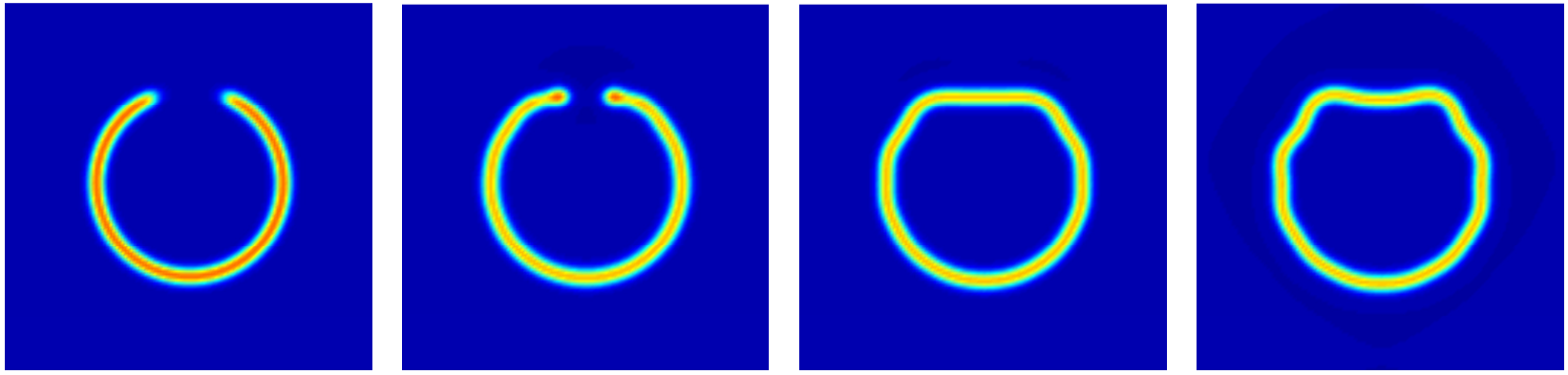

Time= 0 0.2 0.4 0.6

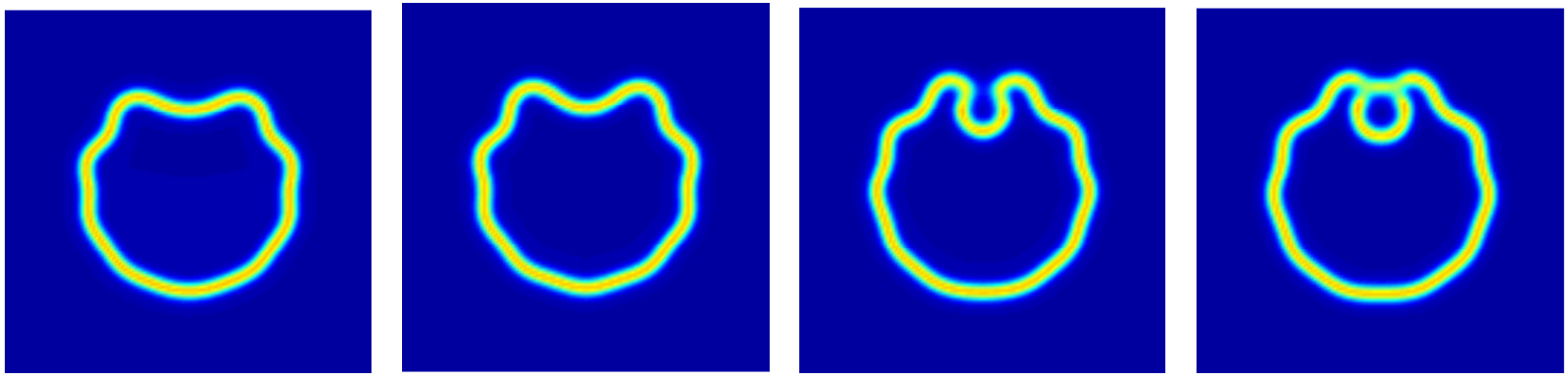

Time= 0.8 1.0 2.0 2.2

Cross sections of a punctured vesicle with too wide initial profile. Meandering induces endocytosis.

Electrostatics and Transport: an Onsager Formulation

Let negative ions be tethered to polymer phase, $n = n(u)$, while counter-ions $p = p(x,t)$ are free to move.

Consider the most general action for electrolyte mixture

$$\mathcal{A} = \int_\Omega \overbrace{k_B T\Big(p\ln p + h(p,n(u))\Big)}^{\text{entropy \& finite volume}} + \overbrace{q_0(p-n)\phi - \frac{1}{2}\overline{\varepsilon}(I,p,n)}^{\text{electrostatic}}\, dx,$$

where h denotes the form of the short-range or finite-volume interactions, q_0 is the elemental charge, $I = |\nabla\phi|$ is electrostatic field intensity, and $\overline{\varepsilon}$ is related to the polarization or displacement field induced by the electric field.

Derive a Poisson equation by requiring ϕ to be a critical point of action

$$\frac{\delta\mathcal{A}}{\delta\phi} := \nabla\cdot\left(\frac{\partial\overline{\varepsilon}}{\partial I}\nabla\phi\right) + q_0(p-n) = 0,$$

in particular the classic orientational permittivity (dielectric) takes the form

$$\varepsilon := \frac{\partial\overline{\varepsilon}}{\partial I} = -2\frac{\delta\mathcal{A}}{\delta I}.$$

Equivalent to the standard derivation of statistical mechanics.

The Free Energy

Substituting for the charge density,

$$p - n = -\frac{1}{q_0}\nabla \cdot (\varepsilon(I, p, n)\nabla\phi)\,,$$

from Poisson's equation in $\mathcal{A}$, defines the electrostatic free energy,

$$\mathcal{E}_{\text{elect}}(\phi, p, n(u)) := \int_\Omega \Big(k_B T(p \ln p + h(p, n)) + \overbrace{I\frac{\partial \overline{\varepsilon}}{\partial I} - \frac{1}{2}\overline{\varepsilon}}^{E\cdot D} \Big)\, dx,$$

which is bounded below if $\overline{\varepsilon}$ is convex in I. Combining the electrostatic energy with the interfacial energy produces a total free energy,

$$\mathcal{T}(u, p, \phi) := \underbrace{\int_\Omega \frac{1}{2}(\epsilon^2 \Delta u - W'(u))^2\, dx}_{\mathcal{F}_0(u)} + \mathcal{E}_{\text{elect}}(u, p, \phi),$$

where $\mathcal{E}_{\text{elect}} = \mathcal{E}_{\text{elect}}(u)$ through $n = n(u)$. The total action is

$$\mathcal{A}_{\mathcal{T}} = \mathcal{F}_0(u) + \mathcal{A}(u, p, \phi).$$

Onsager's Free Energy Dissipation

The gradient flow of the action,

$$u_t = \Delta \frac{\delta \mathcal{A}_\mathcal{T}}{\delta u} = \Delta \left[\frac{\delta \mathcal{F}_0}{\delta u} + \left(k_B T \frac{\partial h}{\partial n} - q_0 \phi - \frac{1}{2} \frac{\partial \bar{\varepsilon}}{\partial n} \right) \frac{\partial n}{\partial u}(u) \right],$$

$$p_t = \frac{D_p}{k_B T} \nabla \cdot \left(p \nabla \frac{\delta \mathcal{A}_\mathcal{T}}{\delta p} \right),$$

which, expanded out becomes a Poisson-Nernst-Planck

$$p_t = D_p \nabla \cdot \Bigg(\left[1 + p \frac{\partial^2 h}{\partial p^2} \right] \nabla p + \overbrace{p \frac{\partial^2 h}{\partial p \partial n} \nabla n(u) + \frac{p}{k_B T} \nabla \left(\phi - \frac{1}{2} \frac{\partial \bar{\varepsilon}}{\partial p} \right)}^{\text{convective}} \Bigg).$$

coupled to Poisson's equation,

$$\nabla \cdot (\varepsilon(I, p, n(u)) \nabla \phi) = q_0 (n - p).$$

The system dissipates the total free energy $\mathcal{T}$,

$$\boxed{\frac{d}{dt} \mathcal{T}(u, p, \phi) = - \left(\int_\Omega \left| \nabla \frac{\delta \mathcal{F}_0}{\delta u} \right|^2 + \frac{D_p}{k_B T} p \left| \nabla \frac{\delta \mathcal{A}_\mathcal{T}}{\delta p} \right|^2 dx \right) \leq 0,}$$

via an Onsager mechanism through the charge density p and the phase field u.

Comparison with the FCH energy

Comparing

$$u_t = \Delta \frac{\delta \mathcal{A}_{\mathcal{T}}}{\delta u} = \Delta \left[\frac{\delta \mathcal{F}_0}{\delta u} + \left(k_B T \frac{\partial h}{\partial n} - q_0 \phi - \frac{1}{2} \frac{\partial \bar{\varepsilon}}{\partial n} \right) \frac{\partial n}{\partial u}(u) \right],$$

with

$$u_t = \Delta \left[\frac{\delta \mathcal{F}_0}{\delta u} + \epsilon^4 \eta_1 \Delta u - \epsilon^2 \eta_2 W'(u) \right],$$

it is tempting to make the associations,

"Quantum surface terms"

$$\eta_1 \epsilon^4 \Delta u \approx -\frac{1}{2} \frac{\partial \bar{\varepsilon}}{\partial n} \frac{\partial n}{\partial u},$$

"Quantum volume terms" $\sim$ finite volume plus bulk electrostatic

$$\eta_2 \epsilon^2 W'(u) \approx \left(q_0 \phi - k_B T \frac{\partial h}{\partial n} \right) \frac{\partial n}{\partial u}.$$

Summary

- Network Morphology can be described, at a phenomenological level, by a continuum system with few (4-5) key parameters
- Numerical simulations corresponding to minutes of real-time evolution are possible
- More sophisticated gradient flows can be developed which couple electrostatics, momentum balance, and interfacial morphology into a gradient flow
- Numerical limitations are still very significant – validation of the models, beyond very rough 'eye-ball' test, will be a significant undertaking.

Acknowledgments

NSF-DMS 0707792
NSF-DMS 0934568 (Solar)
NSF-DMS 0929189 (IGMS)
NSF-DMS 1109127